Recent Astronomical Results from COAST

John S. Young[a], John E. Baldwin[a], Roger C. Boysen[a], Amanda V. George[a], Christopher A. Haniff[a], Craig D. Mackay[b], Debbie Pearson[a], John Rogers[a], Peter J. Warner[a], Donald M. A. Wilson[a], and Richard W. Wilson[a,c]

[a]Astrophysics Group, Cavendish Laboratory, Madingley Road, Cambridge CB3 0HE, UK

[b]Institute of Astronomy, Madingley Road, Cambridge CB3 0HA, UK

[c]On secondment from: UK Astronomy Technology Centre, Royal Observatory, Edinburgh, Blackford Hill, Edinburgh, EH9 3HJ, UK

ABSTRACT

We present the latest astronomical results from the Cambridge Optical Aperture Synthesis Telescope (COAST). COAST is a first-generation stellar interferometer, which uses an array of small (40 cm) separated telescopes to perform high-resolution imaging at visible and near-infrared wavelengths. The new science results from COAST exploit two recently-added capabilities of the COAST array, namely the ability to observe in any of the infrared J, H and K bands as well as at visible wavelengths, plus operation with five telescopes. We present contemporaneous observations of the red supergiant Betelgeuse at three wavelengths in the red and near-infrared. These data show that the apparent symmetry of the stellar disk is a strong function of wavelength, but that the bright spots seen in visible light are consistent with a convective origin. Data obtained using all five array elements on the symbiotic star CH Cygni reveal an elliptical distortion of the disk of the red giant, possibly related to mass transfer to a compact companion.

Keywords: interferometry, closure phase, imaging, infrared, supergiants, symbiotic stars

1. INTRODUCTION

The Cambridge Optical Aperture Synthesis Telescope (COAST) is a first-generation stellar interferometer, which uses an array of small (40 cm) separated telescopes to perform imaging with ten-milliarcsecond resolution at optical and near-infrared wavelengths. The status of COAST was reviewed recently by Baldwin et al.[1] Here we will not attempt to cover all of the more recent developments at COAST, but rather highlight a few which have enabled new astronomical programmes to be carried out, and also present some recent astronomical results from COAST.

Further details of the technical developments at COAST are given in posters by Haniff et al.,[2] George et al.,[3] and Pearson et al.[4]

2. INFRARED IMAGING

2.1. Filter wheel

The infrared correlator[5] at COAST has recently been upgraded by the installation of a filter wheel in the IR camera, permitting rapid switching between five chosen bands in the 1.0–2.4 μm range during the night. Figure 1 shows visibilities measured with COAST at a wavelength of 1.65 μm on the Mira variable star R Cassiopeiae. J band (1.3 μm) data recorded at a very similar phase in the previous pulsation cycle is also shown. The visibilities measured in the two wavebands differ significantly on long baselines ($> 10\,\mathrm{M}\lambda$), indicating different apparent angular sizes and/or limb-darkening profiles. The two wavebands clearly probe different layers in the stratified atmosphere of the Mira variable. Multiple-wavelength observations at this resolution ($\sim$10 mas) should permit atmospheric models to be tested against a sample of cool stars.

Other author information:
J.S.Y.(correspondence): E-mail: J.S.Young@mrao.cam.ac.uk
COAST world-wide-web pages: http://www.mrao.cam.ac.uk/telescopes/coast/

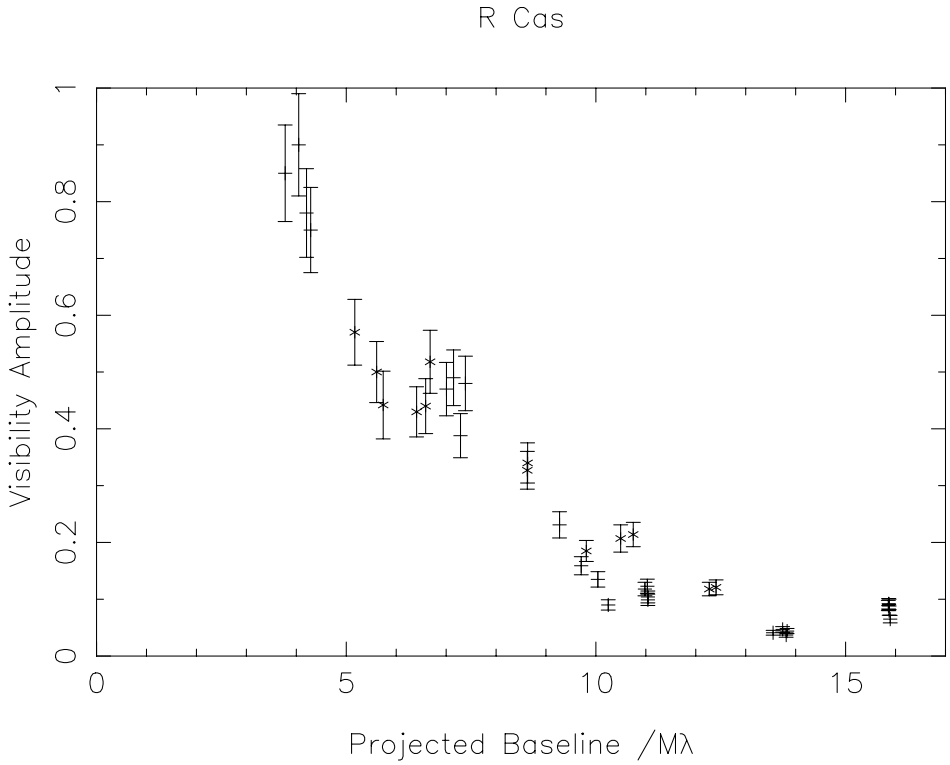

Figure 1. Visibilities for the Mira variable R Cassiopeiae in two infrared wavebands. The vertical crosses are J band ($1.3\,\mu$m) data, and the diagonal crosses are H band ($1.65\,\mu$m) measurements. The data-sets were measured at pulsation phases 0.16 and 1.13 respectively.

2.2. Multiple-wavelength imaging of Betelgeuse

A conclusive demonstration of the value of multiple-wavelength imaging is given by recent COAST observations of the M2 supergiant star Betelgeuse (α Orionis). A fuller report of these results will be published shortly.[6] Previous high-resolution imaging of Betelgeuse, performed exclusively at visible wavelengths, has provided conclusive evidence that its brightness distribution is far from uniform, and in particular has suggested that it can be modelled as a small number of bright unresolved features ('hotspots') superimposed on a symmetric disk.[7–10] The compact features contribute 10–20% of the total flux, and both their locations and intensities change on time-scales of months.[11] There is still no consensus as to the origin of these features (see, e.g. the discussion by Uitenbroek et al.[12]), but the majority of previous workers have interpreted the 'hotspots' as the tops of the giant convection cells predicted by Schwarzshild.[13] In this picture, the bright features should exhibit the spectral behaviour of blackbodies slightly hotter than the stellar disk.

2.2.1. Observations and data reduction

To test the convective hotspot model, contemporaneous visibility amplitude and closure phase data were secured at three widely-spaced wavelengths, on eight nights in October/November 1997. Short-wavelength data were obtained at the William Herschel Telescope on La Palma, by the technique of non-redundant masking. A five-hole mask was inserted in a re-imaged pupil plane to convert the telescope into an interferometer with a maximum baseline of 4 m. The desired bandpasses were selected using interference filters, and had central wavelengths and half-power widths of 700/10 nm and 905/50 nm respectively. Contemporaneous data were recorded at COAST, using a configuration with a maximum baseline of 9 m, to obtain ∼20 milliarcsecond resolution at wavelengths of 905 nm and $1.3\,\mu$m. The optical beam-combiner and avalanche photodiode detectors were used at 905 nm, and the infrared correlator was used for the observations at $1.3\,\mu$m, with a standard J band filter installed in the IR camera. The transmission curve of this filter was slightly modified by telluric absorption, giving an effective wavelength of 1290 nm and a bandwidth of 150 nm. At both COAST and the WHT, observations of Betelgeuse were interleaved with observations

Table 1. Best-fitting models for Betelgeuse in October/November 1997, for wavelengths of 700 nm, 905 nm and 1290 nm respectively. The models consist of a limb-darkened disk, possibly with one or more unresolved bright features superimposed. The coordinates (r, θ) give the position of each unresolved feature (modelled as a finite-sized circular Gaussian) with respect to the centre of the underlying disk. θ is measured North through East. The notation FDD refers to the Hestroffer fully-darkened disk component. For Gaussian components, 'diameter' refers to the FWHM. Parameters for which no uncertainty is quoted were fixed during the fitting process. The uncertainties are 1σ values, and take into account the correlations between the model parameters.

λ (nm)	χ^2	Component	Flux	r (mas)	θ (°)	Diameter (mas)
700	3.0	FDD ($\alpha=4$)	0.68 ± 0.07	–	–	76 ± 5
		Gaussian	0.08 ± 0.02	13.0 ± 1.1	19 ± 4	10
		Gaussian	0.13 ± 0.02	5.9	119	10
		Gaussian	0.09 ± 0.02	12.9 ± 1.1	226 ± 4	10
905	4.3	FDD ($\alpha=4$)	0.95	–	–	71.0 ± 0.7
		Gaussian	0.027 ± 0.003	5.9 ± 1.0	119 ± 5	10
1290	1.8	FDD ($\alpha=1.3 \pm 0.1$)	1.00	–	–	51.4 ± 0.8

of calibrator stars with small and known diameters, to compensate for the effect of changing atmospheric conditions on the measured visibility amplitudes.

Standard methods,[14,15] based on accumulation of the power spectrum and bispectrum, were used to reduce the fringe data from COAST. Each 30–100 s data file yielded a single estimate of the (uncalibrated) visibility amplitude or closure phase. These had formal errors between 2 and 10% of the visibility, and 5–10° respectively. As typically occurs at COAST, the quality of the visibility data was degraded by changes in the seeing conditions between the observations of source and calibrator. Depending upon the proximity on the sky and in time of the source and calibrator observations, additional uncertainties of between 10 and 20% of the visibility were assigned to the data.

Similar procedures[7] were used to obtain visibility amplitudes and closure phases from the WHT data. The uncertainties on the visibilities were again dominated by calibration error, but in this case the errors were unusually large, being ∼30% of the visibility. However, the errors on the closure phases were only 1–3°, giving high sensitivity to the presence of any asymmetric structure on the star.

2.2.2. Results and discussion

We have used model fitting as the most efficient technique for extracting quantitative information about the appearance of the stellar disk from the measured visibilities and closure phases. Some of our data did allow model-independent image reconstructions, and in these cases the recovered images were used to verify the reliability of the model-fitting procedure. The models for the source brightness distribution consisted of either a uniform or limb-darkened disk upon which circular Gaussians were superimposed, to represent bright spots of varying sizes. The limb-darkening parametrisation of Hestroffer[16] was used, which can describe a wide range of limb-darkening using a single parameter α, from uniform disk ($\alpha = 0$) to Gaussian-like profiles ($\alpha \approx 8$). A conjugate gradient algorithm was used to find the best-fitting model parameters, using a range of starting points to increase the chance of finding a global minimum. The models were increased in complexity until an acceptable fit, judged by the minimum χ^2 value, was found.

We find a strong variation in the apparent symmetry of the stellar brightness distribution as a function of wavelength. At 700 nm the star is highly asymmetric, and can be modelled as the superposition of three bright spots on a strongly limb-darkened disk. However, at 905 nm only a single low-contrast feature is visible, and at 1290 nm the star presents a featureless symmetric disk. The parameters of the best-fitting models are given in Table 1, and the corresponding brightness distributions are shown in Figure 2. We emphasise that no single brightness distribution was found to be compatible with any two of the data sets.

We now discuss physical models for the observed asymmetries. The measured change in spot contrast with wavelength is inconsistent with the bright spots being areas of elevated temperature on a blackbody stellar surface. If the disk and hotspots are modelled as blackbodies, all models which give the measured contrast at 700 nm predict

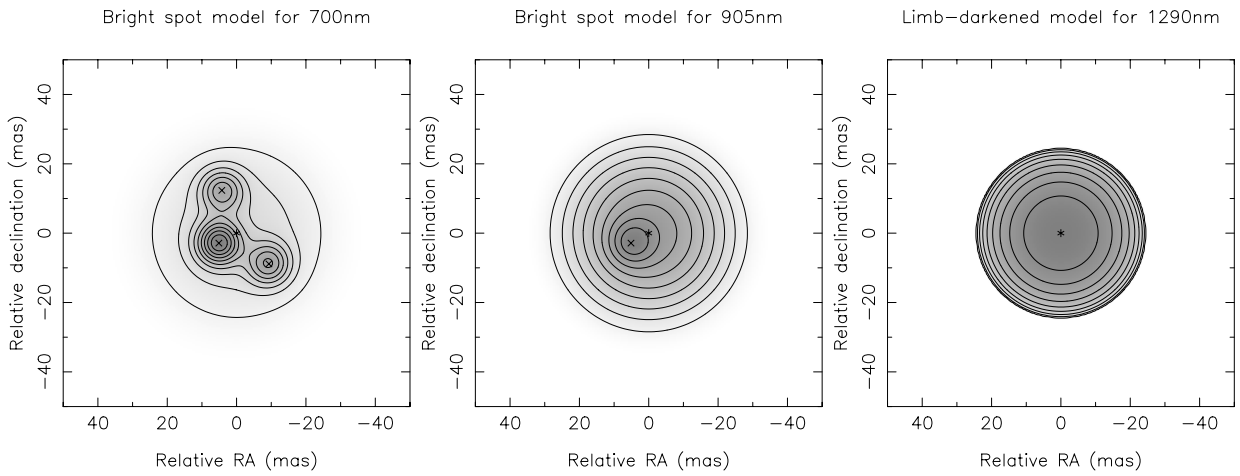

Figure 2. Brightness distributions for the models given in Table 1. From left to right, the models are those for wavelengths of 700 nm, 905 nm, and 1290 nm. The brightest areas are shaded darkest. Note the decrease in asymmetry with wavelength. The sizes of the bright features are unconstrained by the data. To generate these plots, the features were assumed to be Gaussian with FWHM = 10 mas. North is up and East is to the left. The contours are at 10, 20, 30, ..., 90 per cent of the peak brightness.

spot contrasts at least a factor of four greater than those seen at 905 nm and 1290 nm. However, this simple model neglects two effects which are important for these data. First, the apparent diameter of Betelgeuse is a strong function of wavelength,[17] and second, its spectrum cannot be fit by a single blackbody. The first effect was accommodated by fitting uniform disk models to the short baseline visibilities (taking into account the effect of the detected asymmetries), to estimate the effective radiating area at each of our three wavelengths. The effective blackbody flux from the disk component at each wavelength was estimated using a 'typical' M3III spectrum from the catalogue of Pickles[18] (which contains no M2 supergiant spectrum). The relative fluxes and diameter estimates were used to determine effective blackbody temperatures, T_λ, at each wavelength on the assumption that at 1290 nm the star appears as an unobscured blackbody at 3500 K. The resulting T_λ values were $T_{905} = 3230 \pm 10$ K and $T_{700} = 2960 \pm 40$ K. These lower temperatures reflect increased opacity at shorter wavelengths, mostly due to titanium oxide molecules. This first-order correction to the simplest physical model assumes that emission from the hotspots (again modelled as blackbodies) is unobscured.

Values of the hotspot contrast r_λ (equal to the ratio of the flux of a superimposed bright feature to that of the disk component) predicted by this model are compared with the observed values in Table 2. This more realistic model fits the data, but does not permit the size and temperature of the hotspots to be determined independently. If each hotspot covers 10% of the disk area at 700 nm (the largest size compatible with our data), the hotspot temperature is 3500 K. In this limiting case the hotspot temperature is equal to the disk temperature at 1290 nm, i.e. the hotspots are simply regions where the outer atmosphere is transparent. Smaller areas for the hotspots imply that their temperatures must be greater than T_{1290}, and so the bright features do trace pockets of hot gas within the deeper photosphere. If there is some obscuration of the hotspots, the hotspot temperatures derived here must be increased.

Thus the new data *are* consistent with a convective origin for the hotspots. If convective flows perturb the outer atmosphere, which is opaque at shorter wavelengths, they can create more transparent areas through which deeper, hotter layers are seen. At infrared wavelengths, the outer layers are transparent anyway, and a nearly featureless disk is observed. The locations and intensities of the hotspots seen in visible light will evolve with the underlying convective cells.

Two straightforward tests of this scenario are possible. First, at any given epoch, large variations in spot contrast should be seen when crossing deep spectral features, if narrow enough filters (∼5 nm) are used. Second, temporal variations in hotspot contrast should be correlated with changes in TiO band strength, which can easily be measured by narrow-band photometry.

Table 2. Predicted spot-contrasts r_λ for spots with differing fractional areas A_h/A_* as measured at 700 nm and temperatures T_h, computed for a disk temperature of 3500 K at 1290 nm. The effective disk temperature is 3230 K at 905 nm and 2960 K at 700 nm, and the disk diameters are in the ratio 1.00 : 0.81 : 0.72 at 700 nm, 905 nm, and 1290 nm respectively.

A_h/A_*	T_h	r_λ		
at 700 nm		700 nm	905 nm	1290 nm
0.10	3500	0.19	0.031	0.000
0.09	3540	0.19	0.032	0.001
0.08	3600	0.19	0.035	0.004
0.05	3820	0.19	0.038	0.008
0.02	4460	0.19	0.039	0.011
Observed		0.19 ± 0.03	0.028 ± 0.003	< 0.02

3. IMAGING WITH FIVE TELESCOPES

3.1. Introduction

A fifth telescope was installed at COAST in June 1998. This telescope, located on the west arm of the array, may be used interchangeably with another telescope on the same arm. Hence COAST can be switched between two different four-telescope configurations in a few minutes. The addition of the fifth telescope has increased the number of available baselines from six to nine, and the number of closure triangles from four to seven.

The value of this improvement in Fourier plane coverage is demonstrated by COAST observations of the symbiotic star CH Cygni, reported for the first time in these proceedings.

CH Cygni is a member of a class of variable stars with composite spectra, containing features attributable to both a cool M star and a much hotter source. In most symbiotic systems, the high-temperature spectral features originate from matter falling onto a compact companion star. Hinkle et al.[19] classified CH Cygni as a triple system on the basis of precise measurements of the radial velocity of the red giant. In their model, the symbiotic pair, which consists of an M6–7 giant and a white dwarf, has an orbital period of 756 days. Radial velocity measurements from lines probably formed in the white dwarf provide more evidence for this period.[20] The symbiotic pair orbits a third star with period 14.5 yr. There is general agreement on a high inclination for the system. In particular, Skopal and co-workers[21] identified four eclipses consistent with the 756 d period, from U and V band photometry. They also suggested that the third star must also be a red giant, based on evidence for two further eclipses.

Jets were ejected from CH Cygni in 1984, towards the end of a prolonged active phase. These were first seen at radio wavelengths,[22] and subsequently confirmed in the optical.[23,24] The jets were highly collimated, and oriented almost perpendicular to the line of sight.[23] This observation, plus that of eclipses, led to the suggestion that an accretion disk, in a plane normal to the jets, was responsible for their collimation.

We must point out that the 756 d orbital period is not universally accepted, some workers[25,26] preferring an eclipsing binary model with 15.6 yr period, though it would be difficult to accept that such a binary would exhibit symbiotic behaviour.

Garcia[27] attempted to categorise symbiotic stars on the basis of whether the cool star is close to filling its Roche lobe, which determines whether mass transfer takes place via Roche lobe overflow or accretion from a stellar wind. We observed CH Cygni in order to measure any distortion of the red giant's atmosphere, which would be expected if the star falls into the Roche lobe-filling category. If CH Cygni is not a triple system, the size of the $P \sim 15$ yr orbit would preclude Roche-lobe filling, and the red giant's atmosphere would be unlikely to be distorted.

3.2. Observations and data reduction

CH Cygni was observed with COAST on nine nights in August and September 1999, at a wavelength of 905 nm. Details of the observations are given in Table 3. During this period, the two telescopes on the west arm of the interferometer were located on foundations numbered 3 and 4, hence we shall refer to the two possible four-element arrays as the 'w3' and 'w4' arrays. These had maximum baselines of 20 and 22 metres respectively. The Fourier plane coverage for the observations is shown in Figure 3.

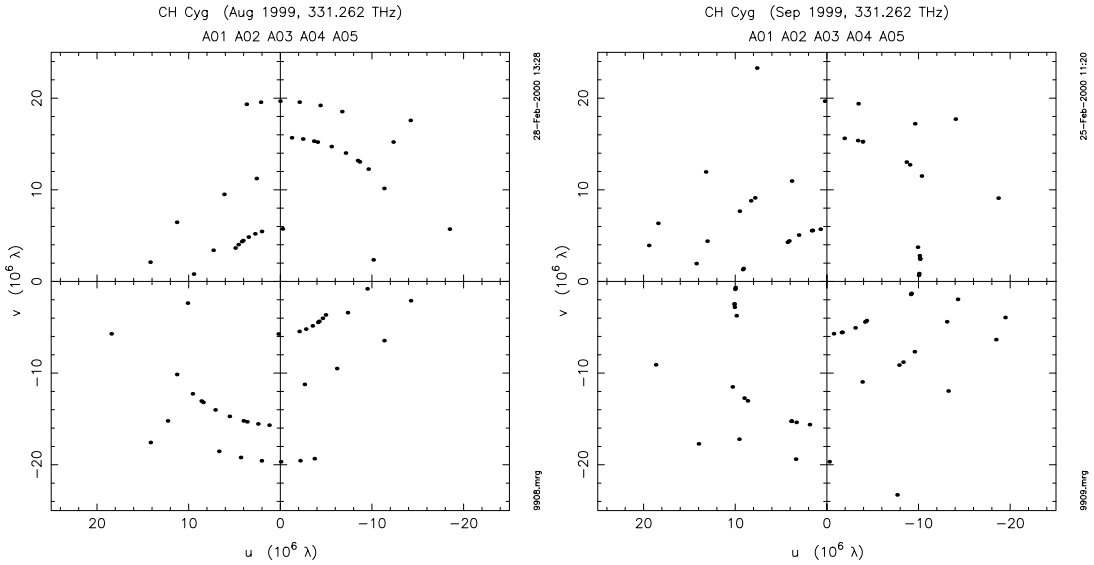

Figure 3. *uv* coverage for the COAST observations of CH Cygni in August (left) and September (right) 1999.

Table 3. Log of observations of CH Cygni. Dates refer to the start of the night of each set of observations. In the second column, 'w3' and 'w4' refer to the two possible choices of four-telescope array (see text). The range of measured baselines is given in the next column. $N_{\rm vis}$ and $N_{\rm cl}$ are the number of visibility and closure-phase measurements made. An identical number of visibility measurements were made for the calibrator star. Each 'measurement' corresponds to 30–100 seconds of observations.

Date	Array(s)	Baseline range (m)	$N_{\rm vis}$	$N_{\rm cl}$
99/08/20	w3	5.6–17.8	6	–
99/08/21	w3	5.5–17.8	10	–
99/08/27	w3	5.2–20.4	18	8
99/09/02	w4	9.6–22.2	5	–
99/09/03	w3, w4	5.2–18.7	8	4
99/09/05	w3	5.2–8.4	2	11
99/09/06	w3	5.3–17.8	5	5
99/09/07	w3	5.3–20.4	11	12
99/09/08	w4	10.9	1	–
99/09/09	w4	9.5–17.6	4	4

The visibility amplitude for CH Cygni was measured on each baseline in turn, to maximise the signal-to-noise of the measurement. On most nights, closure phase data were then secured. Calibration observations of α Lyrae were interspersed at ∼30-minute intervals.

The standard COAST data reduction procedures[14,15] were used to obtain estimates of visibility amplitude and closure phase from the raw fringe data. The main source of error in the final visibilities was calibration error, typically 10% of the visibility. The closure phases on triangles of shorter baselines had errors of ∼2°, which increased to ∼5° when the source was fairly well resolved on one or more baselines.

3.3. Results and discussion

We have again used model-fitting to determine the apparent brightness distribution of CH Cygni. The measured closure phases were all within ∼8° of zero, indicating a nearly centro-symmetric brightness distribution. Consequently

Table 4. Best-fitting models for CH Cygni in August and September 1999. The models consist of a (possibly elliptical) limb-darkened disk, either a Hestroffer model with $\alpha = 1$, or a Gaussian. Position angles are measured North through East. For Gaussian components, 'major axis' refers to the FWHM. Parameters for which no uncertainty is quoted were fixed during the fitting process. The uncertainties are 1σ values, and take into account the correlations between the model parameters.

Epoch	χ^2	Disk type	Major axis (mas)	Axial ratio	Major axis PA (°)
99/08	3.3	Gaussian	6.3 ± 0.1	1.0	–
99/08	2.4	Gaussian	6.7 ± 0.2	0.80 ± 0.06	128 ± 9
99/08	3.1	Hestroffer	10.9 ± 0.2	1.0	–
99/08	1.9	Hestroffer	11.5 ± 0.2	0.84 ± 0.05	126 ± 9
99/09	3.2	Gaussian	6.1 ± 0.1	1.0	–
99/09	1.4	Gaussian	6.6 ± 0.1	0.73 ± 0.04	137 ± 4
99/09	3.1	Hestroffer	10.6 ± 0.2	1.0	–
99/09	1.5	Hestroffer	11.2 ± 0.2	0.79 ± 0.03	136 ± 5

circular or elliptical limb-darkened disk models were employed. The degree of limb-darkening expected at near-continuum wavelengths for a giant in a symbiotic system is uncertain, hence two empirical centre-to-limb profiles were used: a Hestroffer model[16] with $\alpha = 1$, and a Gaussian profile.

In view of the 756 d orbital period, the data from August and from September were treated separately. A circular Hestroffer model gave reduced χ^2 values (ignoring the closure phases, for which the model-predicted values were always zero) of 2.7 and 3.1 for the August and September data respectively, whereas a circular Gaussian model yielded 3.2 for both data-sets. When the disks were allowed to be elliptical, Hestroffer models gave improved χ^2 values of 1.9 and 1.5 for August and September, and Gaussians 2.4 and 1.4. For both data-sets, the direction and degree of ellipticity were independent of the assumed limb-darkening.

The sizes of the calibration errors on the visibilities cannot be estimated with certainty, and so the improved χ^2 values alone do not necessarily imply that the extra free parameters end up fitting any real structure in the data. However, the axial ratios and major axis position angles determined from the independent August and September data-sets *are the same* within the calculated uncertainties, which provides strong evidence that the derived ellipticity is genuine. The value of the fifth COAST telescope is illustrated by the improved constraint on the position angle from the September data compared with that from the August data.

The question of whether the red giant fills its Roche lobe cannot be settled on the basis of the measured angular diameter alone, because of the large uncertainty in the distance to CH Cygni (this uncertainty is much larger than any corrections for limb-darkening or atmospheric extension). The *Hipparcos*[28] trigonometric parallax (from a single-star solution) implies $d = 268^{+79}_{-50}$ pc, and distance estimates in the literature range from 120 pc to 400 pc. Adopting a distance of 250 pc and an angular diameter of 11 mas gives a radius for the red giant of $296 R_\odot$, but this value could be in error by 50%. In comparison, van Belle et al.[29] find the mean radius of four M6 giants to be $148 R_\odot$, with a standard deviation of $41 R_\odot$.

If the orbital plane of the symbiotic pair is seen edge on, the mass function ($0.00140 M_\odot$ for a circular orbit) determined by Hinkle et al.[19] fixes the mass of one component if the other's mass is known. Hence the volume radius (the radius of a sphere with the same volume as the true lobe) of the Roche lobe can be calculated.[30] Hence for a red giant with mass 1–$3 M_\odot$, the Roche lobe radius is in the range 200–$300 R_\odot$. Our measured diameter implies that the red giant in CH Cygni is at least close to filling its Roche lobe.

If the elliptical appearance of CH Cygni was caused by a distortion of the atmosphere of the red giant, Roche lobe filling provides a natural explanation for the distortion. At the time of the observations in August/September 1999 the projected separation of the symbiotic pair in their orbit would have been close to maximum. All plausible mass ratios would give axial ratios $\sim$0.75 for the red giant lobe,[30] consistent with the emitting region tracing a lobe oriented perpendicular to the line of sight. However, the extension is aligned with the jets ejected in 1984, which

would imply that the jets were in the orbital plane, whereas if they were collimated by an accretion disk, we would expect the jets to be *perpendicular* to the orbital plane.

The measured ellipticity may therefore be an extension of the red giant atmosphere perpendicular to the orbital plane. We consider such an extension unlikely. This leaves the possibility that the apparent ellipticity is due to a partial eclipse of the red giant in the symbiotic pair by a second red giant in a 14.5-year orbit. The existence of this red giant companion was proposed by Skopal et al.[21] If the two events identified by Skopal et al. were indeed eclipses, then the two red giants would have been in eclipse at the time of our observations.

3.4. Conclusion

We have measured an apparent ellipticity of the red giant in the symbiotic system CH Cygni. This may be either a distortion of the red giant's atmosphere, possibly related to mass transfer to its symbiotic companion, or an eclipse with the third member of the system. We propose two ways to determine the true cause. First, monitoring of the apparent morphology should reveal either a persistent single disk, or an eclipsing pair of stars. Second, if the accreting material could be mapped, perhaps in Hα, the orientation of the orbital plane would be found.

REFERENCES

1. J. E. Baldwin, R. C. Boysen, C. A. Haniff, P. R. Lawson, C. D. Mackay, J. Rogers, D. St-Jacques, P. J. Warner, D. M. A. Wilson, and J. S. Young, "Current status of COAST," in *Astronomical Interferometry*, R. D. Reasenberg, ed., *Proc. SPIE* **3350**, pp. 736–745, 1998.
2. C. A. Haniff, J. E. Baldwin, R. C. Boysen, A. V. George, D. Pearson, J. Rogers, P. J. Warner, D. M. A. Wilson, and J. S. Young, "New developments at COAST," in *Interferometry in Optical Astronomy*, *Proc. SPIE* **4006**, 2000. These proceedings.
3. A. V. George, J. E. Baldwin, R. C. Boysen, C. A. Haniff, D. Pearson, J. Rogers, P. J. Warner, D. M. A. Wilson, and J. S. Young, "Performance of new fringe-detecting APDs at COAST," in *Interferometry in Optical Astronomy*, *Proc. SPIE* **4006**, 2000. These proceedings.
4. D. Pearson, J. E. Baldwin, R. C. Boysen, A. V. George, C. A. Haniff, J. Rogers, P. J. Warner, D. M. A. Wilson, and J. S. Young, "Channeled spectroscopy at COAST," in *Interferometry in Optical Astronomy*, *Proc. SPIE* **4006**, 2000. These proceedings.
5. J. S. Young, *Infrared Imaging with COAST*. PhD thesis, University of Cambridge, 1999.
6. J. S. Young, J. E. Baldwin, R. C. Boysen, C. A. Haniff, P. R. Lawson, C. D. Mackay, J. Rogers, D. St.-Jacques, P. J. Warner, D. M. A. Wilson, and R. W. Wilson, "New views of Betelgeuse: multi-wavelength surface imaging and implications for models of hotspot generation," *Mon. Not. R. astr. Soc.* , 2000. In press.
7. D. F. Buscher, C. A. Haniff, J. E. Baldwin, and P. J. Warner, "Detection of a bright feature on the surface of Betelgeuse," *Mon. Not. R. astr. Soc.* **245**, pp. 7p–11p, 1990.
8. R. W. Wilson, J. E. Baldwin, D. F. Buscher, and P. J. Warner, "High-resolution imaging of Betelgeuse and Mira," *Mon. Not. R. astr. Soc.* **257**, pp. 369–376, 1992.
9. P. G. Tuthill, C. A. Haniff, and J. E. Baldwin, "Hotspots on late-type supergiants," *Mon. Not. R. astr. Soc.* **285**, pp. 529–539, 1997.
10. V. A. Klückers, M. G. Edmunds, R. H. Morris, and N. Wooder, "Reality and the speckle imaging of stellar surfaces - II. The asymmetry of Alpha Orionis," *Mon. Not. R. astr. Soc.* **284**, pp. 711–716, 1997.
11. R. W. Wilson, V. S. Dhillon, and C. A. Haniff, "The changing face of Betelgeuse," *Mon. Not. R. astr. Soc.* **291**, pp. 819–826, 1997.
12. H. Uitenbroek, A. K. Dupree, and R. L. Gilliland, "Spatially resolved Hubble Space Telescope spectra of the chromosphere of α Orionis," *Astron. J.* **116**, pp. 2501–2512, 1998.
13. M. Schwarzschild, "On the scale of photospheric convection in red giants and supergiants," *Astrophys. J.* **195**, pp. 137–144, 1975.
14. D. Burns, *Experiments with the Cambridge Optical Aperture Synthesis Telescope*. PhD thesis, University of Cambridge, 1997.
15. D. Burns, J. E. Baldwin, R. C. Boysen, C. A. Haniff, P. R. Lawson, C. D. Mackay, J. Rogers, T. R. Scott, P. J. Warner, D. M. A. Wilson, and J. S. Young, "The surface structure and limb-darkening profile of Betelgeuse," *Mon. Not. R. astr. Soc.* **290**, pp. L11–L16, 1997.

16. D. Hestroffer, "Centre to limb darkening of stars: new model and application to stellar interferometry," *Astron. Astrophys.* **327**, pp. 199–206, 1997.
17. Y. Balega, A. Blazit, D. Bonneau, L. Koechlin, R. Foy, and A. Labeyrie, "The angular diameter of Betelgeuse," *Astron. Astrophys.* **115**, pp. 253–256, 1982.
18. A. J. Pickles, "A stellar spectral flux library: 1150-25000 A," *Pub. Astron. Soc. Pac.* **110**, pp. 863–878, 1998.
19. K. H. Hinkle, F. C. Fekel, D. S. Johnson, and W. W. G. Scharlach, "The triple symbiotic system CH Cygni," *Astron. J.* **105**, pp. 1074–1086, 1993.
20. A. Skopal, M. F. Bode, H. M. Lloyd, and H. Drechsel, "IUE high-resolution observations of the symbiotic star CH Cygni: confirmation of the triple-star model," *Astron. Astrophys.* **331**, pp. 224–230, 1998.
21. A. Skopal, M. F. Bode, H. M. Lloyd, and S. Tamura, "Eclipses in the symbiotic system CH Cyg," *Astron. Astrophys.* **308**, pp. L9–L12, 1996.
22. A. R. Taylor, E. R. Seaquist, and J. A. Mattei, "A radio outburst and jet from the symbiotic star CH Cyg," *Nature* **319**, pp. 38–40, 1986.
23. J. Solf, "Optical confirmation and high-resolution spectroscopy of the radio jet from the symbiotic star CH Cygni," *Astron. Astrophys.* **180**, pp. 207–212, 1987.
24. M. F. Bode, J. A. Roberts, R. J. Ivison, J. Meaburn, and A. Skopal, "Echelle spectroscopy of the symbiotic star CH Cygni through quiescence," *Mon. Not. R. astr. Soc.* **253**, pp. 80–88, 1991.
25. J. Mikolajewska, "CH Cygni: double or triple symbiotic system?," in *Interacting Binary Stars*, A. W. Shafter, ed., vol. 56 of *ASP Conference Series*, 1994.
26. U. Munari, B. F. Yudin, E. A. Kolotilov, and T. V. Tomov, "UBV-$JHKLM$ photometry of CH Cygni over 1978-1995: dust properties and doubts on the triple star model," *Astron. Astrophys.* **311**, pp. 484–492, 1996.
27. M. R. Garcia, "Spectroscopic orbits of symbiotic stars: preliminary results," *Astron. J.* **91**, pp. 1400–1415, 1986.
28. *The Hipparcos and Tycho Catalogues*, 1997. ESA SP-1200.
29. G. T. van Belle, B. F. Lane, R. R. Thompson, A. F. Boden, M. M. Colavita, P. J. Dumont, D. W. Mobley, D. Palmer, M. Shao, G. X. Vasisht, J. K. Wallace, M. J. Creech-Eakman, C. D. Koresko, S. R. Kulkarni, and X. P. Pan, "Radii and effective temperatures for G, K, and M giants and supergiants," *Astron. J.* **117**, pp. 521–533, 1999.
30. Z. Kopal, *The Roche Problem*, Kluwer, 1989.